Microbes and Infection

Chlamydia trachomatis relies on the scavenger role of aryl hydrocarbon receptor with detyrosinated tubulin for its intracellular growth, but this is impaired by excess indole

--Manuscript Draft--

Manuscript Number:	MICINF-D-22-00666R1
Article Type:	Original article
Keywords:	Chlamydia trachomatis; indole; IFN-γ; aryl hydrocarbon receptor; cervical swab; AhR-reporter assay; AhR-knockdown cell; scavenger; detyrosinated tubulin
Corresponding Author:	Hiroyuki Yamaguchi Sapporo, JAPAN
First Author:	Saicheng Zhang
Order of Authors:	Saicheng Zhang
	Yuki Funahashi
	Satoho Tanaka
	Torahiko Okubo
	Jeewan Thapa
	Shinji Nakamura
	Hideaki Hideaki
	Hiroyuki Yamaguchi
Manuscript Region of Origin:	JAPAN
Abstract:	Although IFN-γ depletes tryptophan (Trp) as a defense against intracellular Chlamydia trachomatis (Ct) infected to hypoxic vagina, the presence of indole, a precursor of Trp, enables Ct to infect IFN-γ-exposed culture cells. Meanwhile, Trp-derived indole derivatives interact the aryl hydrocarbon receptor (AhR), which is a ligand-dependent transcription factor involved in the cellular homeostasis with tubulin dynamics. Here, the amounts of IFN-γ and indole in cervical swabs with known Ct infection status were measured, and Ct growth in the presence of indole was determined from the perspective of the AhR axis under hypoxia. A positive correlation between the amounts of IFN-γ and indole was found, and both of these amounts were lower in Ct-positive swabs than in Ct-negative ones. Indole as well as other AhR ligands inhibited Ct growth, especially under normoxia. Ct prompted the expression of detyrosinated tubulin (dTTub), but indole inhibited it. Indole did not stimulate the translocation of AhR to nucleus, and it blocked AhR activation in AhR-reporter cells. Ct growth was reduced more effectively under normoxia in AhR-knockdown cells, an effect that was enhanced by indole, which in turn diminished dTTub. Thus, Ct growth relies on the scavenger role of cytosolic AhR responsible for promoting dTTub expression.

Chlamydia trachomatis relies on the scavenger role of aryl hydrocarbon receptor with detyrosinated tubulin for its intracellular growth, but this is impaired by excess indole

Saicheng Zhang[a#], Yuki Funahashi[a#], Satoho Tanaka[a#], Torahiko Okubo[a], Jeewan Thapa[b], Shinji Nakamura[c, d], Hideaki Higashi[e], Hiroyuki Yamaguchi[a]*

[a]Department of Medical Laboratory Science, Faculty of Health Sciences, Hokkaido University, North-12, West-5, Kita-ku, Sapporo 060-0812, Japan

[b]Division of Bioresources, International Institute for Zoonosis Control, Hokkaido University, North-20, West-10, Kita-ku, Sapporo 001-0020, Japan

[c]Division of Biomedical Imaging Research and [d]Division of Ultrastructural Research, Juntendo University Graduate School of Medicine, 2-1-1 Hongo, Bunkyo-ku, Tokyo 113-8421, Japan

[e]Division of Infection and Immunity, International Institute for Zoonosis Control, Hokkaido University, North-20, West-10, Kita-ku, Sapporo 001-0020, Japan

[#]These authors contributed equally to this study.

*__Correspondence:__ Hiroyuki Yamaguchi, Department of Medical Laboratory Science, Faculty of Health Sciences, Hokkaido University, North-12, West-5, Kita-ku, Sapporo 060-0812, Japan

Tel.: +81-11-706-3326; Fax: +81-11-706-3326

E-mail: hiroyuki@med.hokudai.ac.jp

Running title: *Chlamydia trachomatis* intracellular growth and AhR

E-mail addresses:

Saicheng Zhang: zsc1024100319@163.com

Yuki Funahashi: yuki_s2sun.811@icloud.com

Satoho Tanaka: sato_euph_brass0127@eis.hokudai.ac.jp

Torahiko Okubo: t.okubo@hs.hokudai.ac.jp

Jeewan Thapa: jeewan@czc.hokudai.ac.jp

Shinji Nakamura: shinji-n@juntendo.ac.jp

Hideaki Higashi: hidea-hi@czc.hokudai.ac.jp

Hiroyuki Yamaguchi: hiroyuki@med.hokudai.ac.jp

ABSTRACT

Although IFN-γ depletes tryptophan (Trp) as a defense against intracellular *Chlamydia trachomatis* (Ct) infected to hypoxic vagina, the presence of indole, a precursor of Trp, enables Ct to infect IFN-γ-exposed culture cells. Meanwhile, Trp-derived indole derivatives interact the aryl hydrocarbon receptor (AhR), which is a ligand-dependent transcription factor involved in the cellular homeostasis with tubulin dynamics. Here, the amounts of IFN-γ and indole in cervical swabs with known Ct infection status were measured, and Ct growth in the presence of indole was determined from the perspective of the AhR axis under hypoxia. A positive correlation between the amounts of IFN-γ and indole was found, and both of these amounts were lower in Ct-positive swabs than in Ct-negative ones. Indole as well as other AhR ligands inhibited Ct growth, especially under normoxia. Ct prompted the expression of detyrosinated tubulin (dTTub), but indole inhibited it. Indole did not stimulate the translocation of AhR to nucleus, and it blocked AhR activation in AhR-reporter cells. Ct growth was reduced more effectively under normoxia in AhR-knockdown cells, an effect that was enhanced by indole, which in turn diminished dTTub. Thus, Ct growth relies on the scavenger role of cytosolic AhR responsible for promoting dTTub expression.

Keywords:

Chlamydia trachomatis; indole; IFN-γ; aryl hydrocarbon receptor; cervical swab; AhR-reporter assay; AhR-knockdown cell; scavenger; detyrosinated tubulin

Abbreviations

Trp: tryptophan, Ct: *Chlamydia trachomatis*, AhR: aryl hydrocarbon receptor, Tub: tubulin, dTTub: detyrosinated tubulin, EB: elementary body, RB: reticulate body, CtL2: CtL2 434/Bu (a representative lymphogranuloma venereum-causing strain), CtD: CtD/UW-3/CX (a representative urogenital strain), L-K: L-kynurenine, HSP60: heat-shock protein 60, FBS: fetal bovine serum, GFP: green fluorescent protein, ATP: adenosine triphosphate, ROS: reactive oxygen species, IFU assay: inclusion-forming unit assay

1. Introduction

Chlamydia trachomatis (Ct) is an obligate intracellular human pathogenic bacterium with a developmental cycle consisting of elementary body (EB: invasive form) and reticulate body (RB: replicative form) [1]. Through the developmental cycle, Ct survives and replicates within a membrane-bound vacuole, termed the inclusion body [1], which serves as a critical scaffold for successful intracellular modifications such as targeting the energy supply on glycolysis controlled by the PI3K-AKT signaling pathway [2], the cellular trafficking pathways from the Golgi [3], or tubulin (Tub) dynamics [3]. However, the detailed role of this scaffold remains incompletely understood. Meanwhile, Ct is the leading cause of sexually transmitted bacterial infections, with an estimated 131 million new cases of Ct infection annually worldwide [4]. Infection with Ct is also potentially involved in the etiology of cervical cancer [5, 6].

IFN-γ functions as a critical factor in the defense against Ct genital infections by depleting the cellular tryptophan (Trp) pool of the host. However, in *in vitro* experiments, the presence of indole, a Trp precursor, has been shown to rescue genital chlamydiae despite the depletion of Trp in IFN-γ-exposed cells [7]. Therefore, the presence of indole is considered to be associated with the promotion of Ct survival in the vaginal tract [8].

The concentration of indole in the feces of healthy individuals reaches approximately 3 mM [9], and indole can move with gut bacteria into the vaginal tract through the anogenital route [10], suggesting that indole may have a ubiquitous but unidentified role in cellular homeostasis, in addition to its roles as a precursor of tryptophan and in the rescue of Ct against IFN-γ exposure *in vitro*. In fact, high levels of indole derivatives have been reported to ameliorate some inflammatory diseases such as Crohn's disease and type 2 diabetes [11-13]. Interestingly, indole derivatives can act as antibacterial factors against *Legionella pneumophila* [14] and *Mycobacterium tuberculosis* via an unknown mechanism [15, 16]. In addition, indole derivatives can modulate the growth of Ct, potentially through de-repression of the Trp operon by the activation of TrpR [17]. However, the clinical relevance of the amounts of vaginal indole and IFN-γ in Ct infections remains unclear. Furthermore, although the effect of indole on rescuing Ct growth despite the presence of IFN-γ has been emphasized, the negative effect of indole on Ct growth has not been comprehensively investigated.

The aryl hydrocarbon receptor (AhR) is a cytosolic ligand-activated transcription factor responsible for xenobiotic metabolism, which regulates fine-tuning of the mucosal barrier that is responsible for maintaining cellular homeostasis [18]. Trp-derived indole derivatives differentially activate the AhR, which is comprehensively involved in fine-tuning the mucosal barrier [19, 20]. Meanwhile, although AhR promotes transcription by forming a heterodimer with ARNT, it specifically binds to HIF-1α, a master regulator under hypoxia, and induces an adaptive response to hypoxic conditions

[21]. Thus, the amount of AhR in the cytoplasm changes depending on the oxygen conditions, and AhR is more stable in the cytoplasm under hypoxia. This indicates the role of AhR as a scavenger in the cytoplasm under hypoxic conditions preferred by Ct.

AhR is also a factor that determines susceptibility to pathogens. For example, $Ahr^{-/-}$ mice have been shown to be highly susceptible to *Listeria monocytogenes* infection, suggesting that AhR can mitigate bacterial infection [22]. Meanwhile, many Trp metabolites, including indole and its derivatives, which are produced from tissues or the gut microbiota, act as ligands for AhR but exhibit differences in terms of activating it [23]. Some indole derivatives, such as indole-3-carbinol and indole-3-propionic acid, have been reported to induce cell death, impairing the intracellular growth of certain pathogens [24, 25]. Against this background, Ct likely promotes the scavenger role of AhR of removing certain harmful molecules such as Trp-derived indole derivatives from the cytoplasm of host cells. Activation of the AhR can also stimulate adaptive mechanisms for ensuring cellular survival through the Wnt-β-catenin, NF-κB, and/or PI3K-AKT signaling pathways [26], which are frequently targeted by the intracellular parasite Ct [2, 27]. Interestingly, the dynamics of AhR in cells has been reported to be specifically associated with cell cycle arrest or tubulin assembly [4]. In particular, Ct strongly stimulates tubulin recycling by promoting the process of detyrosination of Tub (dTTub) [3]. However, the role of AhR in the intracellular growth of Ct required for Tub dynamics is not completely understood.

In the present study, we measured the amounts of IFN-γ and indole in cervical swabs (*n*=570) obtained from pregnant women with known Ct infection status [28]. We also investigated the intracellular growth of Ct in the presence of pure indole under hypoxia from the perspective of the AhR axis and tubulin dynamics by using AhR reporter cells and AhR-knockdown cells.

2. Materials and Methods

2.1. Collection of endocervical swabs for measuring IFN-γ and indole derivatives

This study used frozen endocervical swabs that had been collected from pregnant women (*n*=570, age: 28.46 ± 5.14, collection period: June 2016 to February 2018) at Toho Obstetrics and Gynecology Hospital in previous studies [28], along with the results of analysis on the status of Ct infection. The amount of IFN-γ was measured with the Human IFN-γ ELISA MAX Deluxe Set (BioLegend, San Diego, CA, USA). The amount of indole derivatives was evaluated using the Kovacs method [9]. Both values were expressed as the amount per total protein.

2.2. Ct strains

Two Ct strains (CtL2: L2/434/Bu and CtD: D/UW-3/CX) were used in this study. Green fluorescent protein (GFP)-expressing transformed CtL2 was established following a previous protocol [29], which was the main strain used in this study. These bacteria were propagated into immortal human epithelial HEp-2 cells and stored at −80°C until use [2]. The cells were maintained in D-MEM (Sigma, St. Louis, MO, USA) containing inactivated 10% fetal bovine serum (FBS) based on our previous study [2].

2.3. Assessment of AhR activation

Immortal hepatic HEp-G2 Lucia AhR cells (InvivoGen, San Diego, CA, USA) with or without CtL2 infection were cultured in the presence or absence of L-K with or without indole for 48 h under normoxia (21% O_2) or hypoxia (2% O_2). The luciferase activity of the culture supernatants was measured with Quanti-Luc™ (InvivoGen), following the manufacturer's protocol. Data are expressed as fold change relative to the control value. The cells were maintained in Opti-MEM (Thermo Fisher, Waltham, MA, USA) containing inactivated 10% FBS.

2.4. Establishment of AhR-knockdown cells

Transient AhR-knockdown HEp-2 cells were established by 24-h transfection of cells with siRNA (AM16708) purchased from Thermo Fisher. As a control, *in vitro* negative

control siRNA (4390843) was also purchased from the same company. Transfection of siRNA (or control siRNA) into cells was performed with a transfection reagent, Lipofectamine RNAiMAX (Thermo Fisher), in accordance with the manufacturer's protocol as described below. Transfection complexes were prepared by incubating 100 μL of Opti-MEM (Thermo Fisher) consisting of 0.8 μL of RNAiMAX and each siRNA (6 pmol) for 30 min at room temperature. After incubation, total transfection complexes were added to HEp-2 cells seeded the day before at 1×10^4 cells into 500 μL of Opti-MEM, and then incubated for 24 h at 37°C in 5% CO_2. After incubation, the cells were infected with CtL2 and incubated in RPMI1640 (Sigma) containing inactivated 10% FBS for 48 h. The amounts of AhR as well as HSP60 and Tub (including dTTub) were confirmed by western blotting.

2.5. Infection and assessment of bacterial numbers

Cells (HEp-2 cells, AhR-reporter HEp-G2 cells, or AhR-knockdown HEp-2 cells) were inoculated with CtL2 (or CtD) at a multiplicity of infection (MOI) of 5–25 and then cultured in the presence or absence of drugs [indole (Sigma, St. Louis, MD, USA), CH-223191 (Sigma), L-kynurenine (L-K; InvivoGen, San Diego, CA, USA), and/or cycloheximide (Sigma)] for 48 h under 21% (normoxia) or 2% (hypoxia) O_2 conditions. Hypoxia was created using a dedicated MIC-101 chamber (Billups-Rothenberg, Del Mar, CA, USA). The numbers of bacterial progeny were determined using the inclusion-forming unit (IFU) assay, in accordance with our previous study [2].

2.6. Assessment of cytotoxicity

The cytotoxic effects of indole, CH-223191, L-K, and the combination of indole and L-K on HEp-2 cells were evaluated with a Cell Counting Kit-8, in accordance with the manufacturer's protocol (Dojindo, Kumamoto, Japan).

2.7. Imaging

Cells were treated with 4% paraformaldehyde in phosphate-buffered saline (PBS), and then permeabilized with 0.1% Triton-X100. After blocking with PBS containing 3% skimmed milk and 0.05% Tween20, cells were stained with primary antibodies [anti-dTTub antibody (ab48389; Abcam, Cambridge, UK), anti-AhR antibody (ab190797; Abcam), or anti-Tub (CLT9002; Cedarlane, Burlington, Ontario, Canada)], followed by secondary antibodies. After washing with PBS containing 0.05% Tween20, the stained cells were mounted with DAPI solution and then observed using a confocal laser (TCSSP5, Leica) or conventional (BZX800, Keyence) fluorescence microscopes. The translocation of AhR to the nucleus and the density of dTTub were determined by the following method. Each image was converted to grayscale; for the imaging of cytosolic AhR, nucleus area was subtracted for the AhR image. Grayscale density on each image was determined with ImageJ (version 1.53K), which was shown as DAPI staining intensity per cell. In addition, the numbers of inclusion bodies formed due to

the infection with GFP-expressing CtL2 were automatically counted by an image analyzer in a microscope system (BZ810; Keyence, Osaka, Japan).

2.8. Western blotting

Cells were lysed in RIPA buffer containing 0.1% SDS (08714-04; Nacalai Tesque, Kyoto, Japan), in accordance with the manufacturer's protocol. The protein samples separated on a 6% separation gel by SDS-PAGE were transferred to a PVDF membrane by semi-dry electroblotting using the Trans-Blot® Turbo™ blotting system (Bio-Rad, Hercules, CA, USA). After blocking with 3% skimmed milk in Tris-buffered saline (TBS) with 0.1% Tween 20, membranes were incubated with primary antibody [anti-aryl hydrocarbon receptor antibody (ab190797; Abcam, Cambridge, UK), anti-HSP60 antibody (sc-57840; Santa Cruz Biotechnology, Dallas, TX, USA), anti-dTTub, or anti-Tub] overnight at 4 °C. After washing with TBS-T, the membranes were incubated with each secondary antibody for 6 h at 4 °C. After washing, the membranes were developed with Clarity™ Western ECL substrate (Bio-Rad) and visualized using ChemiDoc™ XRS (Bio-Rad). Band densities were quantified by ImageJ.

2.9. Statistical analysis

Correlations were analyzed by Spearman's correlation coefficient rank test.

Comparisons between two groups were performed by Student's t-test, while the Bonferroni–Dunn test or Tukey–Kramer test was used for multiple groups. A *p*-value of < 0.05 was considered statistically significant.

3. Results

3.1. Indole derivatives, as well as IFN-γ, had a role in protecting against Ct infection in the vaginal tract

The amounts of IFN-γ and indole derivatives were measured in cervical swabs (n=570) obtained from pregnant women with known Ct infection status [28]. A significant correlation was identified between the amounts of IFN-γ and indole derivatives in the swabs (r=0.947 p<0.0001), regardless of whether the swabs were Ct-positive (n=35, r=0.839, p<0.0001) or -negative (n=535, r=0.948, p<0.0001) (Fig. 1A). Interestingly, the IFN-γ and indole-derivative levels in the Ct-positive swabs (n=35) were significantly lower than in the Ct-negative ones (n=535) (indole: p<0.0001; IFN-γ: p=0.0004) (Fig. 1B and C). Although these results were inconsistent with previous *in vitro* experiments in which indole derivatives were shown to have a positive effect on the survival of Ct in the vaginal tract [7, 8], our findings suggested that indole derivatives, as well as IFN-γ, have a role in the protection against Ct infection in the

vaginal tract. The findings also imply that host factors, such as AhR, which can bind to indole or its derivatives [19, 20], play a biological role in Ct growth.

3.2. Indole inhibited the intracellular growth of Ct (L2 434/Bu and D/UW-3/CX) in HEp-2 cells

The effect of indole on the intracellular growth of Ct [CtL2 (434/Bu, a representative lymphogranuloma venereum-causing strain) and CtD (D/UW-3/CX, a representative urogenital strain)] in HEp-2 cells was assessed. Imaging analysis showed that the number of CtL2 clusters formed in the infected cells, referred to as inclusion bodies [1], was significantly decreased in the presence of indole [21% O_2: 200–1000 μM ($p<0.05$); 2% O_2: 500 and 1000 μM ($p<0.05$)], in a concentration-dependent manner (Fig. 2A). Similarly, the estimated numbers of CtL2 bacteria (EB) with IFUs were significantly lower in the presence of indole than in its absence [21% O_2: 200–1000 μM ($p<0.05$); 2% O_2: 500 and 1000 μM ($p<0.05$)], and the effect was concentration-dependent (Fig. 2B). Meanwhile, under normoxia, lower concentrations of indole inhibited the growth of Ct more efficiently (Fig. 2B), indicating that the effect of indole varies depending on the oxygen concentration. Furthermore, indole (125–500 μM) had an inhibitory effect on the growth of CtD ($p<0.05$) (Fig. S1), although there was no difference in the growth among various O_2 conditions, consistent with previous reports [30]. Additionally, no cytotoxicity of indole toward HEp-2 cells was observed at the concentrations used (20–1000 μM) (Fig. S2). These results indicated that indole significantly inhibited the

growth of Ct strains in immortal epithelial HEp-2 cells more efficiently under normoxia.

3.3. Indole derivatives [indole, AhR antagonist (CH-223191), L-kynurenine (L-K)] had a protective role against Ct (L2 434/Bu) via impairing the scavenger role of AhR in AhR-reporter cells

To confirm the involvement of AhR in the inhibitory effect of indole, the effect of CH-223191, an antagonist of AhR [31], on the growth of CtL2 was first evaluated. CH-223191 (2.5–10 μM) significantly inhibited the intracellular growth of CtL2 more efficiently under normoxia ($p<0.05$) (Fig. S3). No cytotoxicity of CH-22319 on HEp-2 cells was observed at the concentrations used (2.5–10 μM) (Fig. S4). Next, we assessed whether indole itself could block AhR activation by L-K, an agonist of AhR with an indole backbone [18], using HEp-G2 AhR reporter cells. Indole significantly inhibited the activation of AhR in the reporter cells (Fig. 3A). However, neither indole nor the CtL2 infection itself stimulated activation of the AhR signal (Fig. 3B). Stimulation with L-K (25 and 100 μg/ml) significantly inhibited the intracellular growth of CtL2 in HEp-2 cells ($p<0.05$), in a concentration-dependent manner (Fig. 3C). Imaging analysis also revealed that, in contrast to the stimulation with L-K, indole did not promote the translocation of AhR to the nucleus, regardless of the oxygen conditions (Fig. S5 and Fig. S6). Meanwhile, the addition of a high concentration of L-K exerted cytotoxic effects on HEp-2 cells regardless of CtL2 infection (Fig. S7), and the presence of cycloheximide, which specifically inhibits protein synthesis in eukaryotes, did not affect

the inhibitory effect of indole on CtL2 infection (Fig. S8). In line with this, it has been shown that, unlike other Cts, the intracellular growth of CtL2 itself is not affected by treatment with cycloheximide [32]. The above results clearly indicate that the growth of CtL2 requires cytosolic AhR itself to act as a scavenger to sequester the substrates, but does not require AhR signaling.

3.4. Indole inhibited the production of dTTub as well as Ct (L2 434/Bu) growth

As mentioned above, the dynamics of AhR in cells is crucially associated with cell cycle arrest or tubulin assembly [4], and Ct strongly stimulates Tub recycling by promoting the production of dTTub [3]. Therefore, to confirm the role of cytosolic AhR in CtL2 growth via tubulin dynamics, the change of dTTub amount was compared in the presence or absence of indole by using imaging analysis with antibody specific to dTTub. The results showed that Ct strongly promoted the expression of dTTub around the inclusion bodies, but it was clearly suppressed in a manner dependent on the indole concentration (Fig. 4 and Fig. S9), identically supported by the observation with a confocal laser fluorescence microscope that denies the association of aberrant bodies of CtL2 to the inhibitory mechanism of indole (Fig. 5). On the other hand, no difference was observed in the staining pattern of Tub regardless of the presence or absence of Indole (Fig. S10). The results suggested that AhR is involved in regulating Tub recycling to support the intracellular growth of CtL2.

3.5. The growth of Ct (L2 434/Bu) was inhibited with a decrease of dTTub in AhR-knockdown cells

Finally, to confirm the role of AhR in the intracellular growth of CtL2 required for tubulin dynamics, we constructed transient AhR-knockdown HEp-2 cells using siRNA and assessed whether this knockdown affected the growth of CtL2 and the amount of dTTub in these cells. As shown in Fig. 6, successful silencing of AhR was confirmed by western blotting (Fig. 6A and B, “AhR” and “AhR/Tub”). Similarly, the amounts of HSP60 (heat-shock protein 60) correlating with the growth of CtL2 were significantly diminished more effectively in the knockdown cells under normoxia (Fig. 6A and B, “HSP60” and “HSP60/Tub”). In addition, the amount of dTTub was significantly inhibited more effectively in the knockdown cells under normoxia (Fig. 6A and B, “dTTub” and “dTTub/Tub”). Interestingly, the AhR-knockdown cells resulted in a slight increase of Tub amounts in hypoxic condition (Fig. S11), although the mechanism remains unknowns. Moreover, the IFU numbers of CtL2 were significantly suppressed in the AhR-knockdown cells, supporting the results of western blotting (Fig. S12). These results consistently indicated that the intracellular growth of CtL2 relies on AhR itself, which plays a scavenger role in sequestering harmful Trp-derived indole derivatives more efficiently under hypoxia, while controlling Tub dynamics.

4. Discussion

Indole derivatives have been detected in human feces at a concentration of approximately 3 mM [9]. Similarly, our data indicated that indole was present in cervical swabs at concentrations in the range of 0.3–6.64 mM. However, because the method using Kovacs reagent as applied in this study is not specific for detecting pure indole [9], our results reflect the level of indole and its derivatives. There are three major pathways of Trp metabolism for the production of indole: gut microbiota [33], the kynurenine pathway [34], and the serotonin production pathway [35]. In addition, the amount of indole produced by commensal *Escherichia coli* has been shown to reach approximately 600 μM [36]. Given that indole is clearly the dominant component relative to its derivatives, the inhibitory effect of indole derivatives on Ct growth was determined by an *in vitro* experiment using pure indole.

From the clear findings of decreases in both the number of bacteria (EB) and the size of inclusion bodies formed in HEp-2 cells, the replication of Ct in the host cells was significantly diminished by indole in a dose-dependent manner. This clearly ruled out the possibility of a transition to Ct persistence, with Ct division and proliferation being stopped but its viability being maintained [37]. Meanwhile, indole did not exert any cytotoxicity on HEp-2 cells, and thus the inhibition was unlikely to be associated with cell-death responses such as apoptosis by stopping the supply of ATP to Ct. In support

of this, no activation of pro-caspase 3 responsible for the initiation of apoptosis was identified, even upon culture with a high level of indole (~1000 μM) (data not shown).

Indole, a ligand of AhR, has been considered to play a critical role in AhR-signal transduction responsible for maintaining cellular or tissue homeostasis [18-21]. However, contrary to our expectations, indole itself significantly inhibited the activation of AhR with L-K in AhR-reporter cells, and no activation of AhR with indole itself was seen in the reporter cells. In fact, the presence of indole did not promote the translocation of AhR to the nucleus, suggesting the role of cytosolic AhR. Several studies have also indicated that certain molecules with an aromatic hydrocarbon structure similar to indole or their combinations can induce cytotoxicity and inflammation in cells in a manner dependent on ROS generation, which typically occurs in the cytosol [38-40]. These findings indicate that indole clearly has dual functions: causing tissue damage and controlling AhR overexpression. Thus, Ct relies on the scavenger role of cytosolic AhR to sequester indole itself or presumably its derivatives to suppress unknown harmful biological responses.

Some indole derivatives de-repress the trp operon by displacing tryptophan from TrpR, a repressor of this operon [41, 42]. In the absence of indole, this process generates pyruvate with ammonia, killing Ct [41, 42]. However, our experiments were generally performed in the presence of excess indole. Because Ct clearly failed to proliferate successfully in AhR-knockdown cells, the TrpR de-repression-mediated bactericidal

effect is limited in our experiments. Meanwhile, because some studies have shown that indole derivatives play roles as antibacterial factors against *L. pneumophila* [43, 44] and *M. tuberculosis* [45], intracellular parasitic bacteria may universally require AhR for their growth to sequester substances that inhibit such growth within the cell.

Assembled tubulins are critical components of the cytoskeleton, playing various roles, including in cellular migration, mitosis, mechanical stress, cell polarity, and intracellular transport, which are crucially regulated by the tubulin detyrosination cycle [46]. Meanwhile, after infection, Ct surrounded by a membrane-bound vacuole (inclusion body) migrates to the vicinity of the Golgi apparatus with the motor protein that moves on tubulin and develops. Tubulin dynamics is thus crucial for the successful intracellular growth of Ct [3, 47]. Meanwhile, we found that indole clearly decreased the amount of dTTub, which was enhanced by Ct infection, although it did not affect the amount of Tub expression itself. This indicates that cytosolic AhR plays a role in maintaining tubulin dynamics by inducing dTTub during the intracellular growth of CtL2. In addition, interestingly, AhR silencing resulted in a slight increase of Tub amounts, suggesting that AhR may be involved in the regulation of dTTub through controlling the stable expression of Tub with complexity.

The effect of indole on the intracellular proliferation of Ct appears to be more efficient under normoxia. As mentioned above, AhR requires the formation of a heterodimer with ARNT for transcription [21, 48]. However, HIF-1α, a master regulator under hypoxia,

preferentially requires the heterodimer with ARNT for transcription under hypoxic conditions [21, 48]. Under hypoxia, the amount of AhR in the cytoplasm is likely to be high and its scavenger effect may be efficiently maintained, providing a favorable environment for the intracellular growth of Ct. In fact, our previous studies clearly demonstrated that Ct favors intracellular environments for its growth under hypoxia [49]. In addition, because the intracellular growth of Ct is regulated by cellular signal modifications by more than 70 effector molecules that are transported into the cytoplasm using a type III secretion system [2, 50], some of these effectors might interact with the AhR to stabilize its scavenger role in the cytoplasm by promoting tubulin dynamics.

In conclusion, we demonstrated that, contrary to our understanding based on previous studies [7, 8], vaginal indole as well as IFN-γ has a protective role against the intracellular growth of Ct. Furthermore, although the details of this inhibitory effect remain unclear, our *in vitro* studies showed that the blockade of cytosolic AhR by excess Trp-derived indole causing the decrease of dTTub is the mechanism underlying the impaired intracellular growth of Ct. Thus, our findings clearly indicate that Ct relies on the scavenger role of cytosolic AhR with dTTub, but this is easily impaired by the presence of excess indole (Fig. 7). This study highlights the need to consider the pathogenicity of not only Ct but also other pathogenic bacteria from the perspective of the indole and AhR axis.

Acknowledgments

We thank Mr. Keisuke Taki (Hokkaido University Hospital), Dr. Junji Matsuo (Health Sciences University of Hokkaido), and Dr. Furuta (Hokkaido University) for assisting this study. A proofreading company, Edanz (https://jp.edanz.com/ac), edited a draft of this manuscript.

Author Contributions

H.Y. conceived and designed the study. S.Z., Y.F., S.T., T.O., and J.T. performed the laboratory work. S.Z., Y.F., S.T., and S.N. analyzed the data with imaging. H.H. and H.Y. established the GFP-expressing Ct. H.Y. wrote the manuscript with revision by J.T.

Declaration of Competing Interests

We have no conflicts of interest in association with the present study.

Funding

This study was funded by Grants-in-Aid for Scientific Research, KAKENHI (grant numbers: 16H05225 and 21H02726) (to H.Y.). The funders had no role in the study design, data collection and analysis, decision to publish, or preparation of the manuscript.

Ethical approval

All of the subjects provided written informed consent to participate in this study. This study was approved by the ethics committees of both Toho Obstetrics and Gynecology Hospital and the Faculty of Health Sciences, Hokkaido University (15-99-5).

Appendix: Supplementary data

Fig. S1: Effect of indole on the intracellular growth of the CtD strain under normoxic and hypoxic conditions. HEp-2 cells were infected with CtD (MOI10), and then incubated in the presence or absence of indole (125–500 μM) for 48 h. After incubation, the IFUs were measured. The left and right graphs show the kinetics of the IFUs under normoxia and hypoxia, respectively. Data are shown as the mean ± SD. The experiment was performed at least three times. *$p < 0.05$ vs. control.

Fig. S2: Cytotoxic effects of indole (0–1000 μM) on HEp-2 cells under normoxia (upper panel) and hypoxia (lower panel), evaluated with a Cell Counting Kit-8. Plots (n=6) are shown as the mean ± SD of the percentage (%) relative to the untreated cells (indole: "0"). IC_{50}, 50% inhibitory concentration.

Fig. S3. Effect of CH-223191 (AhR antagonist) on the intracellular growth of CtL2 under normoxic (left panel) and hypoxic conditions (right panel). HEp-2 cells were infected with CtL2 (MOI5), and then incubated in the presence or absence of CH-223191 for 48 h. After incubation, inclusion numbers (upper and middle panels) and IFUs (lower panels) were measured. Upper images show representative images of the inclusions. Scale bars represent 500 μm. Heatmaps (middle panels) show the inclusion numbers relative to the control. Data are shown as the mean ± SD. The experiment was performed at least three times. *$p < 0.05$ vs. control.

Fig. S4: Cytotoxic effects of CH-223191 (0–20 μM) on HEp-2 cells under normoxic (upper panel) and hypoxic conditions (lower panel), evaluated with a Cell Counting Kit-8. Plots (*n*=6) show the mean ± SD of the percentage (%) relative to untreated cells. IC_{50}, the 50% inhibitory concentration. *$p < 0.05$ vs. control ("0") without the drug (left plot).

Fig. S5: Representative images showing the changes of AhR location due to the stimulation with or without AhR ligands (**A**) and the integrated density of the nucleus per cell (%) (**B**) under normoxia. GFP-expressing CtL2 infected HEp-2 cells and the infected cells were then incubated in the presence or absence of AhR ligands [indole (500 μM) and L-K (25 μg/mL)] under normoxia. After 48 h of incubation, the cells were stained with antibodies specific to AhR and Tub (see the Materials and Methods). Green (strong), CtL2. Green (weak), Tub. Red, AhR. Blue, nucleus (DAPI). Scale bars represent 20 μm. *$p<0.05$, vs. Control [CtL2(-)]. #$p<0.05$, vs. Control [CtL2(+)]. $$p<0.05$, vs. L-K[CtL2(-)]. &p<0.05, vs. L-K[CtL2(+)]. Bars show each of the images with distinct cell numbers. *n*, total cell numbers counted.

Fig. S6: Representative images showing the changes of AhR location due to the stimulation with or without AhR ligands (**A**) and the integrated density of nucleus per cell (%) (**B**) under hypoxia. See the legend of Fig. S4.

Fig. S7: Cytotoxic effects of L-K (0–25 μg/mL) with or without indole (0-500 μM) on

HEp-2 cells in the presence [white bars: CT(+)] or absence [black bars: CT(–)] of CtL2 infection under normoxic (upper panel) and hypoxic conditions (lower panel), evaluated with a Cell Counting Kit-8 48 h after incubation. Bars (n=6) are shown as the mean ± SD of the percentage (%) relative to untreated cells. The dotted lines marked with IC_{50} show the 50% inhibitory concentration. *$p < 0.05$ vs. control [L-K(-)/Indole(-)] without each of the drugs (left bars).

Fig. S8: Effects of cycloheximide (2 μg/mL) on the growth inhibition of CtL2 by the treatment with indole (200 μM) in HEp-2 cells. Cells were cultured for 48 h under normoxia or hypoxia, and collected for the assessment of bacterial numbers by IFU assay.

Fig. S9: Effect of indole on maintaining the amount of dTTub in CtL2-infected HEp-2 cells. GFP-expressing CtL2 infected HEp-2 cells and the infected cells were then incubated in the presence or absence of indole (200 or 500 μM) under normoxia and hypoxia. After 48 h of incubation, the cells were stained with antibodies specific to dTTub, and the converted grayscale densities were calculated with ImageJ (see the Materials and Methods). n, total cell numbers counted. *p<0.05, vs. Control.

Fig. S10: Representative confocal laser microscopic images showing the changes of Tub amounts due to the stimulation with or without indole. HEp-2 cells were infected with or without GFP-expressing CtL2 and the infected cells were then incubated in the

presence or absence of indole (200 or 500 μM) under normoxia (A) and hypoxia (B). After 48 h of incubation, the cells were assessed by imaging using a conventional microscope (BZX800, Keyence) with an antibody specific to Tub (see the Materials and Methods). Green, CtL2. Red, Tub. Blue, nucleus (DAPI). Scale bars represent 10 μm.

Fig. S11: Effect of AhR knockdown in cells on the expression of Tub with CtL2 infection in the presence or absence of indole under normoxia or hypoxia through western blotting analysis. The band density of Tub in Fig. 6 was reused and then compared between AhR knockdown cells (AhRsi) and non-AhR knockdown cells (Contsi). "AhRsi" and "Contsi" show the mean [Indole(+)/(-)] ± SD under normoxia or hypoxia. *$p < 0.05$ vs. Contsi of each oxygen condition.

Fig. S12: Representative images showing the inclusion formation of CtL2 and the IFU number comparison between AhRsi and Contsi in the presence [Indole(+), 500 μM] or absence of indole [Indole(-)]. Data representing IFU numbers are shown as the mean ± SD. The experiment was performed three times. Scale bar, 200 μm. *$p < 0.05$ vs. Contsi Indole(-). #$p < 0.05$.

References

1. Hammerschlag MR. The intracellular life of chlamydiae. Semin Pediatr Infect Dis 2002;13:239-248.
2. Thapa J, Hashimoto K, Sugawara S, Tsujikawa R, Okubo T, Nakamura S, et al. Hypoxia promotes *Chlamydia trachomatis* L2/434/Bu growth in immortal human epithelial cells via activation of the PI3K-AKT pathway and maintenance of a balanced NAD(+)/NADH ratio. Microbes Infect 2020;22:441-450.
3. Al-Zeer MA, Al-Younes HM, Kerr M, Abu-Lubad M, Gonzalez E, Brinkmann V, Meyer TF. *Chlamydia trachomatis* remodels stable microtubules to coordinate Golgi stack recruitment to the chlamydial inclusion surface. Mol Microbiol 2014;94:1285-1297.
4. O'Connell CM, Ferone ME. *Chlamydia trachomatis* Genital Infections. Microb Cell 2016;3:390-403.
5. Yang X, Siddique A, Khan AA, Wang Q, Malik A, Jan AT, et al. *Chlamydia trachomatis* infection: their potential implication in the etiology of cervical cancer. J Cancer 2021;12:4891-4900.
6. Karim S, Souho T, Benlemlih M, Bennani B. Cervical Cancer Induction Enhancement Potential of Chlamydia Trachomatis: A Systematic Review. Curr Microbiol 2018;75:1667-1674.
7. Nelson DE, Virok DP, Wood H, Roshick C, Johnson RM, Whitmire WM, et al. Chlamydial IFN-gamma immune evasion is linked to host infection tropism. Proc Natl Acad Sci USA 2005;102:10658-10663.

8. Aiyar A, Quayle AJ, Buckner LR, Sherchand SP, Chang TL, Zea AH, et al. Influence of the tryptophan-indole-IFNgamma axis on human genital *Chlamydia trachomatis* infection: role of vaginal co-infections. Front Cell Infect Microbiol 2014;4:72.

9. Darkoh C, Chappell C, Gonzales C, Okhuysen P. A rapid and specific method for the detection of indole in complec biological samples. Appl Environ Microbiol 2015;81:8093-8097.

10. Taki K, Watanabe T, Matsuo J, Sakai K, Okubo T, Matsushita M, et al. Impact of bacterial traces belonging to the *Enterobacteriaceae* on the prevalence of *Chlamydia trachomatis* in women visiting a community hospital in Japan. J Infect Chemother 2018;24:815-821.

11. Wlodarska M, Luo C, Kolde R, d'Hennezel E, Annand JW, Heim CE, et al. Indoleacrylic acid produced by commensal *Peptostreptococcus* species suppresses inflammation. Cell Host Microbe 2017;22:25–37.e6.

12. de Mello VD, Paananen J, Lindström J, Lankinen MA, Shi L, Kuusisto J, et al. Indolepropionic acid and novel lipid metabolites are associated with a lower risk of type 2 diabetes in the Finnish Diabetes Prevention Study. Sci Rep 2017;7:46337.

13. Gao J, Xu K, Liu H, Liu G, Bai M, Peng C, et al. Impact of the gut microbiota on intestinal immunity mediated by tryptophan metabolism. Front Cell Infect Microbiol 2018;8:13.

14. Inoue H, Yajima Y, Kawano G, Nagasawa H, Sakuda S. Isolation of indole-3-aldehyde as a growth inhibitor of *Legionella pneumophila* from Diaion HP-20 resins used to culture the bacteria. Biocontrol Sci 2004;9:39–41.

15. Negatu DA, Liu JJJ, Zimmerman M, Kaya F, Dartois V, Aldrich CC, et al, Whole-cell screen of fragment library identifies gut microbiota metabolite indole propionic acid as antitubercular. Antimicrob Agents Chemother 2018;62:e01571-17.
16. Kaufmann SHE. Indole propionic acid: A small molecule links between gut microbiota and tuberculosis. Antimicrob Agents Chemother 2018;62:e00389-18.
17. Sherchand SP, Aiyar A. Ammonia generation by tryptophan synthase drives a key genetic difference between genital and ocular *Chlamydia trachomatis* isolates. Proc Natl Acad Sci USA 2019;116:12468-12477.
18. Rothhammer V, Quintana FJ. The aryl hydrocarbon receptor: an environmental sensor integrating immune responses in health and disease. Nat Rev Immunol 2019;19:184-197.
19. Nieves KM, Hirota SA, Flannigan KL. Xenobiotic receptors and the regulation of intestinal homeostasis: harnessing the chemical output of the intestinal microbiota. Am J Physiol Gastrointest Liver Physiol 2022;322:G268-G281.
20. Stockinger B, Shah K, Wincent E. AHR in the intestinal microenvironment: safeguarding barrier function. Nat Rev Gastroenterol Hepatol 2021;18:559-570.
21. Vorrink SU, Domann FE. Cite Share. Regulatory crosstalk and interference between the xenobiotic and hypoxia sensing pathways at the AhR-ARNT-HIF1α signaling node. Chem Biol Interact 2014;218:82-8.
22. Shi LZ, Faith NG, Nakayama Y, Suresh M, Steinberg H, Czuprynski CJ. The aryl hydrocarbon receptor is required for optimal resistance to *Listeria monocytogenes* infection in mice. J Immunol 2007;179:6952-6962.

23. Denison MS, Faber SC. And Now for Something Completely Different: Diversity in Ligand-Dependent Activation of Ah Receptor Responses. Curr Opin Toxicol 2017;2:124-131.

24. Lim HM, Park SH, Nam MJ. Induction of apoptosis in indole-3-carbinol-treated lung cancer H1299 cells via ROS level elevation. Hum Exp Toxicol 2021 ;40:812-825.

25. Kwun MS, Lee DG. Investigation of distinct contribution of nitric oxide and each reactive oxygen species in indole-3-propionic-acid-induced apoptosis-like death in *Escherichia coli*. Life Sci 2021;285:120003.

26. Akhtar S, Hourani S, Therachiyil L, Al-Dhfyan A, Agouni A, Zeidan A, et al. Epigenetic Regulation of Cancer Stem Cells by the Aryl Hydrocarbon Receptor Pathway. Semin Cancer Biol 2021;S1044-579X(20)30184-X.

27. Kintner J, Moore CG, Whittimore JD, Butler M, Hall JV. Inhibition of Wnt Signaling Pathways Impairs *Chlamydia trachomatis* Infection in Endometrial Epithelial Cells. Front Cell Infect Microbiol 2017;7:501.

28. Thapa J, Watanabe T, Isoba M, Okubo T, Abe K, Minami K, et al. *Chlamydia trachomatis* isolated from cervicovaginal samples in Sapporo, Japan, reveals the circulation of genetically diverse strains. BMC Infect Dis 2020;20:53.

29. Bauler LD, Hackstadt T. Expression and targeting of secreted proteins from *Chlamydia trachomatis*. J Bacteriol 2014;196:1325-1334.

30. Juul N, Jensen H, Hvid M, Christiansen G, Birkelund S. Characterization of *in vitro* chlamydial cultures in low-oxygen atmospheres. J Bacteriol 2007;189:6723-6726.

31. Kim SH, Henry EC, Kim DK, Kim YH, Shin KJ, Han MS, et al. Novel compound 2-methyl-2H-pyrazole-3-carboxylic acid (2-methyl-4-o-tolylazo-phenyl)-amide (CH-223191) prevents 2,3,7,8-TCDD-induced toxicity by antagonizing the aryl hydrocarbon receptor. Mol Pharmacol 2006;69:1871-1878.

32. Reed SI, Anderson LE, Jenkin HM. Use of cycloheximide to study independent lipid metabolism of *Chlamydia trachomatis* cultivated in mouse L cells grown in serum-free medium. Infect Immun 1981;31:668-673.

33. Zelante T, Iannitti RG, Cunha C, De Luca A, Giovannini G, Pieraccini G, Zecchi R, D'Angelo C, Massi-Benedetti C, Fallarino F, Carvalho A, Puccetti P, Romani L. Tryptophan catabolites from microbiota engage aryl hydrocarbon receptor and balance mucosal reactivity via interleukin-22. Immunity 2013;39:372-385.

34. Clarke G, Grenham S, Scully P, Fitzgerald P, Moloney RD, Shanahan F, Dinan TG, Cryan JF. The microbiome-gut-brain axis during early life regulates the hippocampal serotonergic system in a sex-dependent manner. Mol Psychiatry 2013;18:666-673.

35. Yano JM, Yu K, Donaldson GP, Shastri GG, Ann P, Ma L, Nagler CR, Ismagilov RF, Mazmanian SK, Hsiao EY. Indigenous bacteria from the gut microbiota regulate host serotonin biosynthesis. Cell 2015;161:264-276.

36. Domka J, Lee J, Wood TK. YliH (BssR) and YceP (BssS) regulate *Escherichia coli* K-12 biofilm formation by influencing cell signaling. Appl Environ Microbiol 2006;72:2449-2459.

37. Witkin SS, Minis E, Athanasiou A, Leizer J, Linhares IM. *Chlamydia trachomatis*: the Persistent Pathogen. Clin Vaccine Immunol 2017;24:e00203-17.

38. Vogel CFA, Van Winkle LS, Esser C, Haarmann-Stemmann T. The aryl hydrocarbon receptor as a target of environmental stressors - Implications for pollution mediated stress and inflammatory responses. Redox Biol 2020;34:101530.

39. Chen G, Huo X, Luo X, Cheng Z, Zhang Y, Xu X. E-waste polycyclic aromatic hydrocarbon (PAH) exposure leads to child gut-mucosal inflammation and adaptive immune response. Environ Sci Pollut Res Int 2021;28:53267-53281.

40. Andersen MHG, Saber AT, Pedersen JE, Pedersen PB, Clausen PA, Løhr M, Kermanizadeh A, Loft S, Ebbehøj NE, Hansen ÅM, Kalevi Koponen I, Nørskov EC, Vogel U, Møller P. Assessment of polycyclic aromatic hydrocarbon exposure, lung function, systemic inflammation, and genotoxicity in peripheral blood mononuclear cells from firefighters before and after a work shift. Environ Mol Mutagen 2018;59:539-548.

41. Sherchand SP, Aiyar A. Ammonia generation by tryptophan synthase drives a key genetic difference between genital and ocular *Chlamydia trachomatis* isolates. Proc Natl Acad Sci USA 2019;116:12468-12477.

42. Pokorzynski ND, Hatch ND, Ouellette SP, Carabeo RA. The iron-dependent repressor YtgR is a tryptophan-dependent attenuator of the *trpRBA* operon in *Chlamydia trachomatis*. Nat Commun 2020;11:6430.

43. Grossowicz N Phytohormones as specific inhibitors of *Legionella pneumophila* growth. Isr J Med Sci 1990;26:187–190.

44. Inoue H, Yajima Y, Kawano G, Nagasawa H, Sakuda S Isolation of indole-3-aldehyde as a growth inhibitor of *Legionella pneumophila* from Diaion

HP-20 resins used to culture the bacteria. Biocontrol Sci 2004;9:39–41.

45. Kaufmann SHE Indole propionic acid: A small molecule links between gut microbiota and tuberculosis. Antimicrob Agents Chemother 2018;62:e00389-18.

46. Nieuwenhuis J, Brummelkamp TR. The Tubulin Detyrosination Cycle: Function and Enzymes. Trends Cell Biol 2019;29:80-92.

47. XX Campbell S, Richmond SJ, Yates PS. The effect of *Chlamydia trachomatis* infection on the host cell cytoskeleton and membrane compartments. J Gen Microbiol 1989;135:2379-2386.

48. Mandl M, Depping R. Hypoxia-inducible aryl hydrocarbon receptor nuclear translocator (ARNT) (HIF-1β): is it a rare exception? Mol Med 2014;20:215-20.

49. Thapa J, Yoshiiri G, Ito K, Okubo T, Nakamura S, Furuta Y, Higashi H, Yamaguchi H. *Chlamydia trachomatis* Requires Functional Host-Cell Mitochondria and NADPH Oxidase 4/p38MAPK Signaling for Growth in Normoxia. Front Cell Infect Microbiol 2022;12:902492.

50. Bugalhão JN, Mota LJ. The multiple functions of the numerous *Chlamydia trachomatis* secreted proteins: the tip of the iceberg. Microb Cell 2019;6:414-449.

Figure Legends

Fig. 1. Relationship of IFN-γ with indole in the presence or absence of Ct infection in the cervical tract. **A.** Correlation between the amounts of IFN-γ and indole in cervical swabs obtained from pregnant women (*n*=570) with (red, *n*=35) and without (gray, *n*=535) Ct infection. Each plot shows the amount per total protein. The *r* values are the correlation coefficients. **B.** Comparison of the amounts of indole in Ct-negative swabs (gray bar, *n*=535) and Ct-positive swabs (red bar, *n*=35). Bars represent the average amount per total protein with the SD. **C.** Comparison of the amounts of IFN-γ in Ct-negative swabs (gray bar, *n*=535) and Ct-positive swabs (red bar, *n*=35). Bars show the average amount per protein with the SD.

Fig. 2. Effects of indole on the intracellular growth of CtL2 under conditions of normoxia and hypoxia. HEp-2 cells were infected with Ct (MOI5), and then incubated in the presence or absence of indole (20–1000 μM) for 48 h. After incubation, the inclusion numbers and IFUs were measured. **A.** Assessment of the inclusion numbers. Left panels show representative images of the inclusions. Scale bars represent 20 μm. PC, phase contrast. Right graphs show the kinetics of the inclusions with heatmaps (inclusion numbers are relative to the control). Data are shown as the mean ± SD. The experiment was performed at least three times. *$p < 0.05$ vs. control. **B.** Assessment of the IFU numbers. The left and right graphs show the kinetics of IFUs in the presence of indole under normoxia and hypoxia, respectively. Data are shown as the mean ± SD. The experiment was performed at least three times. *$p < 0.05$ vs. control.

Fig. 3. Association of AhR with the inhibitory effect of indole on the intracellular growth of CtL2. **A.** Effects of indole (200 and 500 μM) on activation of the AhR signal by L-K (25 μg/ml) under normoxia and hypoxia. The activation of AhR was assessed by using HEp-G2 AhR-reporter cells (see the Materials and Methods). Data (fold change) are shown as the mean ± SD. The experiment was performed at least three times. *$p < 0.05$ vs. control; #$p < 0.05$ vs. L-K. **B.** Effects of CtL2 infection (MOI5 and MOI25) on activation of the AhR signal with L-K (25 μg/ml) under normoxia and hypoxia. The activation of AhR was assessed by using HEp-G2 AhR-reporter cells (see the Materials and Methods). Data (fold change) are shown as the mean ± SD. The experiment was performed at least three times. *$p < 0.05$ vs. control. #$p < 0.05$ vs. L-K. **C.** Effect of L-K (25 μg/ml) on the intracellular growth of CtL2 (MOI1 and MOI5) under normoxia and hypoxia. Data (IFU/ml) are shown as the mean ± SD. The experiment was performed at least three times. *$p < 0.05$ vs. control; #$p < 0.05$ vs. L-K.

Fig. 4. Representative conventional microscopic images showing the changes of dTTub amounts due to the stimulation with or without indole. HEp-2 cells were infected with or without GFP-expressing CtL2 and the infected cells were then incubated in the presence or absence of indole (200 or 500 μM) under normoxia (A) and hypoxia (B). After 48 h of incubation, the cells were assessed by imaging using a conventional microscope (BZX800, Keyence) with an antibody specific to dTTub (see the Materials and Methods). Green, CtL2. Red, dTTub. Blue, nucleus (DAPI). Scale

bars represent 20 μm.

Fig. 5. Representative confocal laser microscopic images showing the changes of dTTub amounts due to the stimulation with or without indole. HEp-2 cells were infected with or without GFP-expressing CtL2 and the infected cells were then incubated in the presence or absence of indole (500 μM) under normoxia (A) and hypoxia (B). After 48 h of incubation, the cells were assessed by imaging using a confocal laser microscope (TCSSP5, Leica) with an antibody specific to dTTub (see the Materials and Methods). Green, CtL2. Red, dTTub. Blue, nucleus (DAPI). Scale bars represent 10 μm.

Fig. 6. Effect of AhR knockdown in cells on the intracellular growth of CtL2 through western blotting analysis. The amounts of three distinct targets [HSP60 (CtL2 growth), AhR, and dTTub] were compared between AhR-knockdown cells (AhRsi) and normal HEp-2 cells (Contsi) in the presence [Indole(+), 500 μM] or absence of indole [Indole(-)] under normoxia (**A**) and hypoxia (**B**). The experiment was performed in triplicate. Data (fold change) representing band density normalized with tubulin are shown as the mean ± SD. Black, gray, and dotted bars show AhR (AhR/Tub), HSP60 (HSP60/Tub), and dTTub (dTTub/Tub), respectively. #$p < 0.05$ vs. Indole(-) in Contsi and AhRsi. *$p < 0.05$ vs. Contsi Indole(-).

Fig. 7. A model showing the molecular mechanism behind the inhibitory effect of

indole on CtL2 growth via the scavenger role of AhR itself.

Figure1

Fig. 1

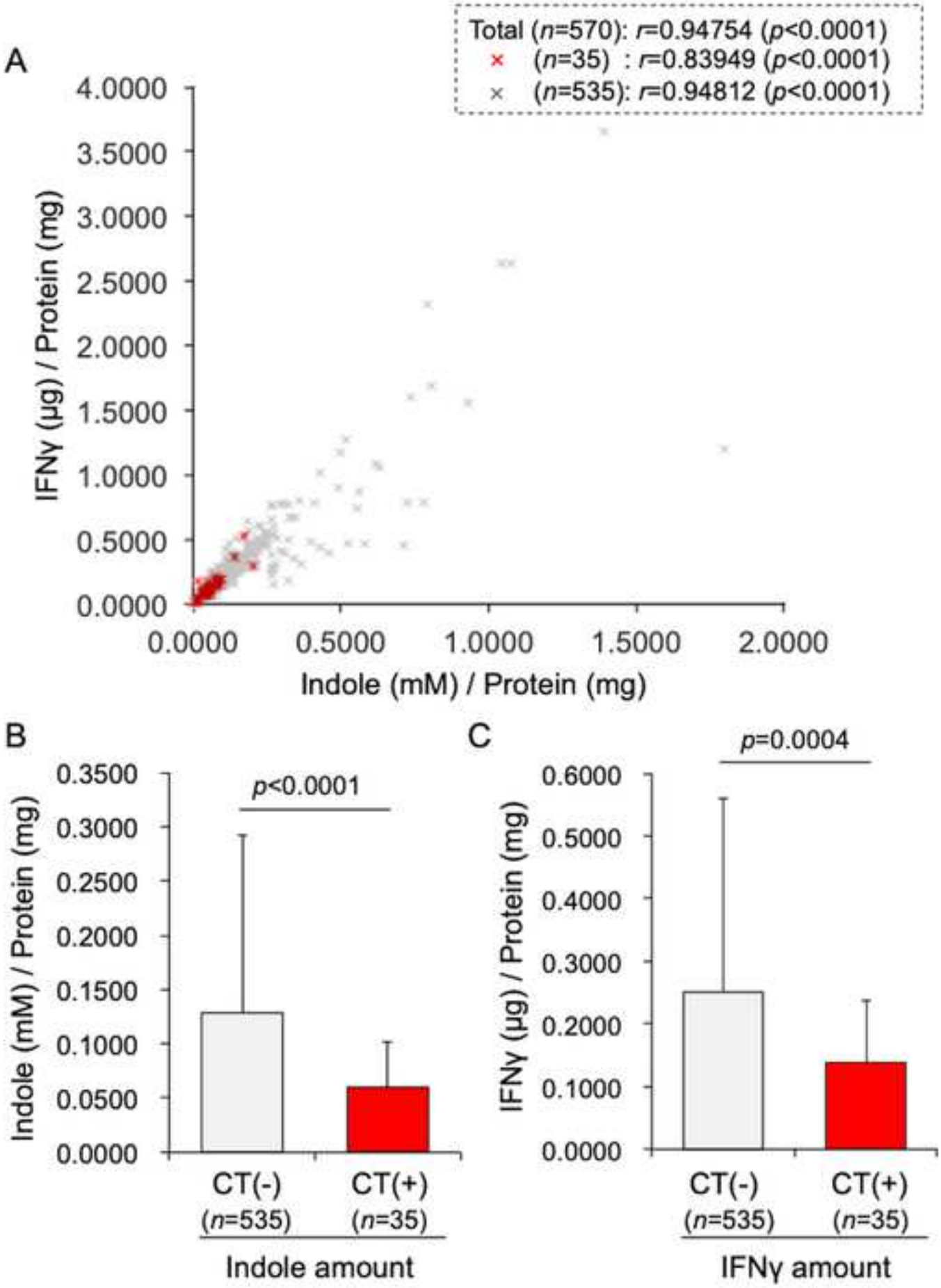

Figure2

Fig. 2

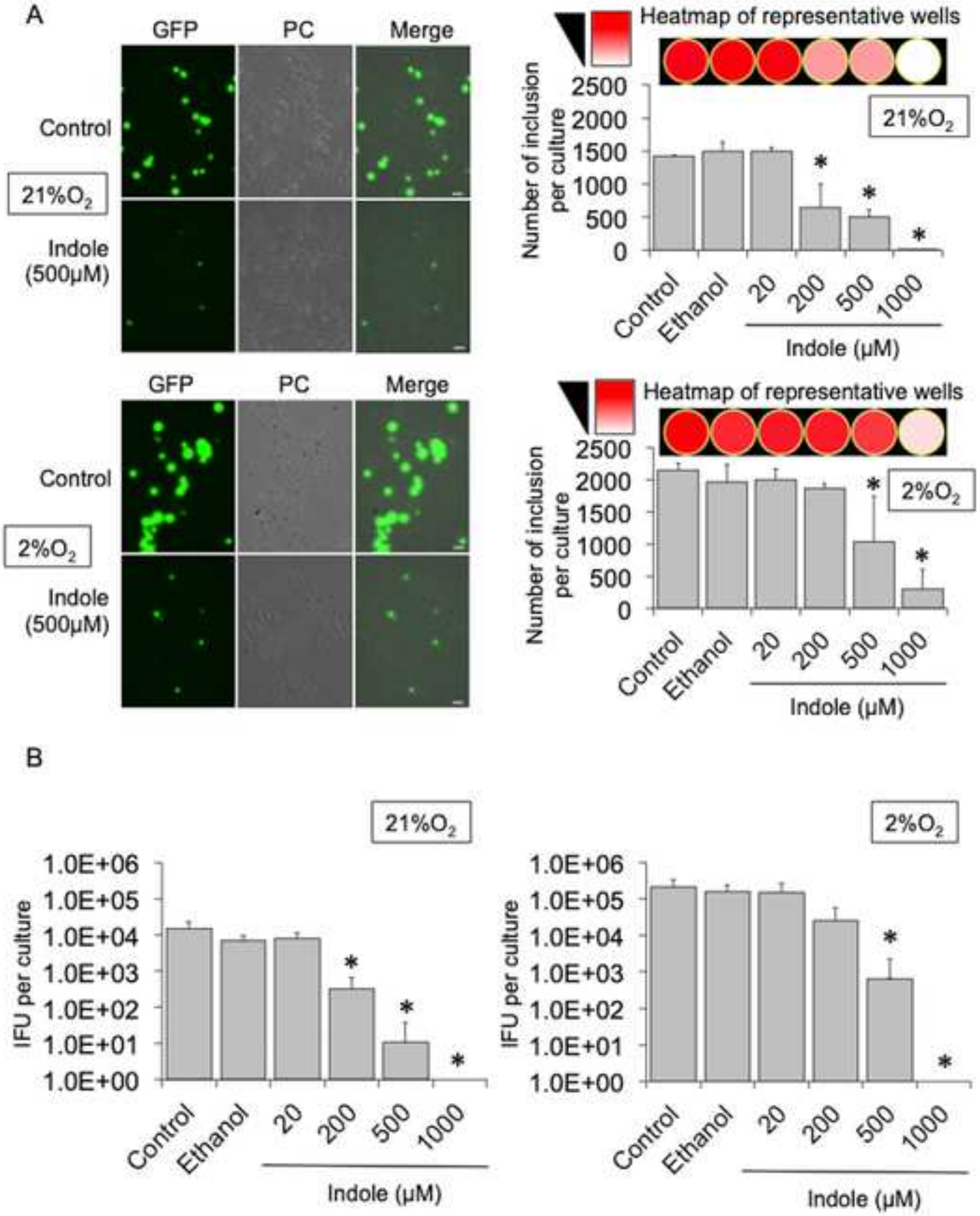

Figure3

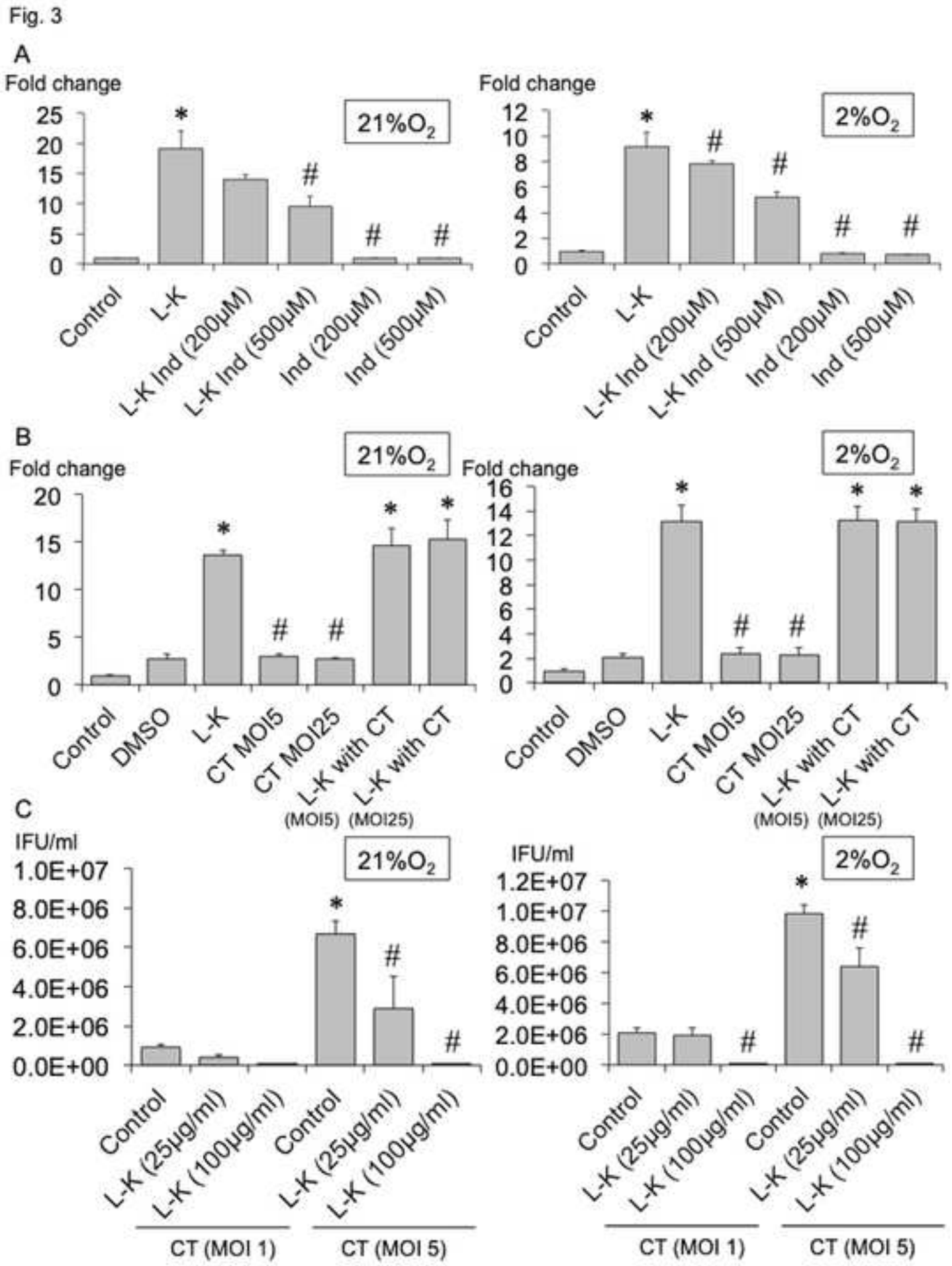
Fig. 3
A
Fold change
21%O2
25
20
15
10
5
0
Control
L-K
L-K Ind (200μM)
L-K Ind (500μM)
Ind (200μM)
Ind (500μM)
Fold change
2%O2
12
10
8
6
4
2
0
B
Fold change
21%O2
20
15
10
5
0
Control
DMSO
L-K
CT MOI5
CT MOI25
L-K with CT (MOI5)
L-K with CT (MOI25)
Fold change
2%O2
16
14
12
10
8
6
4
2
0
C
IFU/ml
21%O2
1.0E+07
8.0E+06
6.0E+06
4.0E+06
2.0E+06
0.0E+00
Control
L-K (25μg/ml)
L-K (100μg/ml)
CT (MOI 1)
CT (MOI 5)
IFU/ml
2%O2
1.2E+07
1.0E+07
8.0E+06
6.0E+06
4.0E+06
2.0E+06
0.0E+00

Figure4

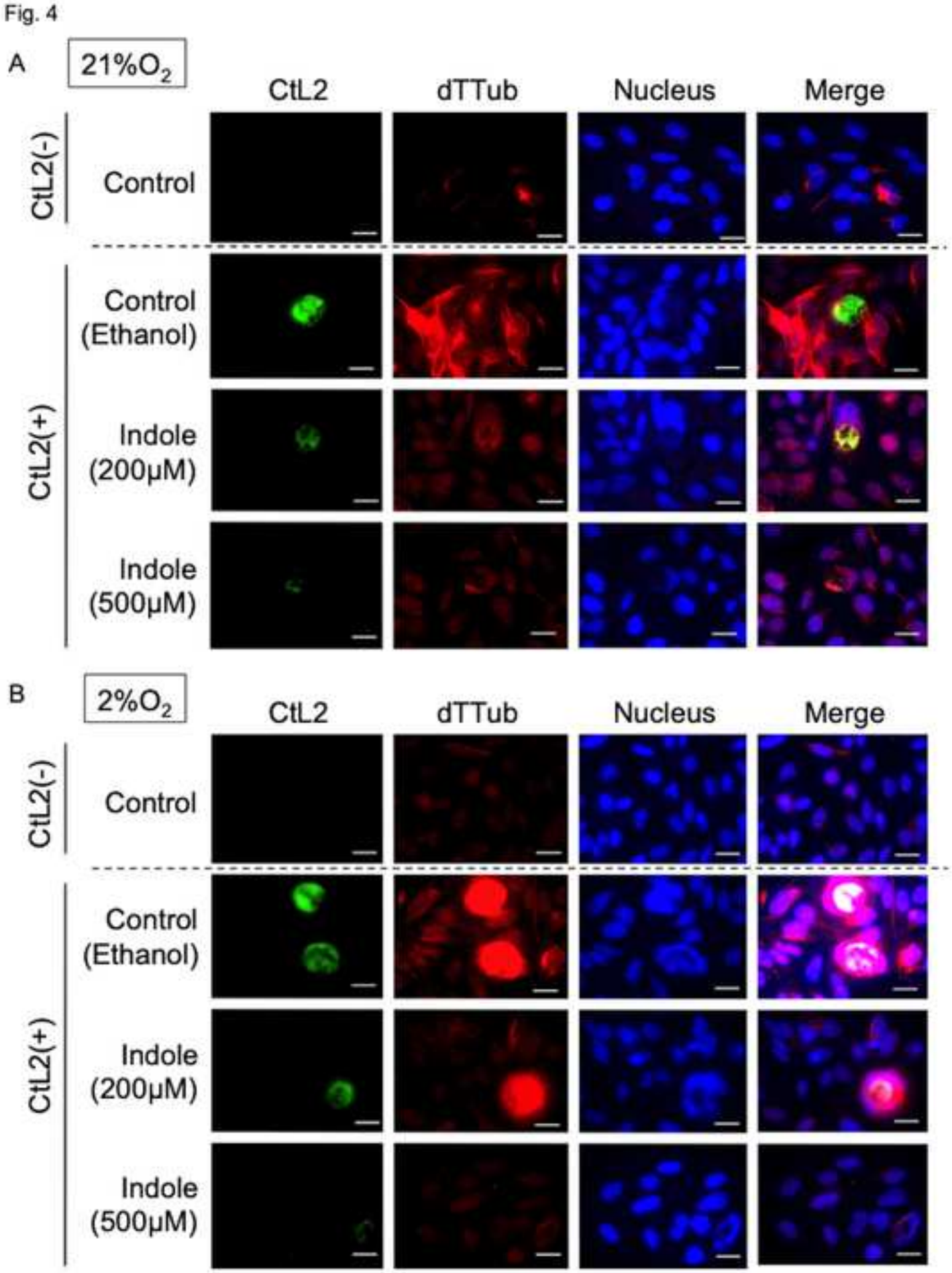
Fig. 4
A
21%O2
CtL2
dTTub
Nucleus
Merge
CtL2(-)
Control
CtL2(+)
Control (Ethanol)
Indole (200μM)
Indole (500μM)
B
2%O2
CtL2
dTTub
Nucleus
Merge
CtL2(-)
Control
CtL2(+)
Control (Ethanol)
Indole (200μM)
Indole (500μM)

Figure5

Fig. 5

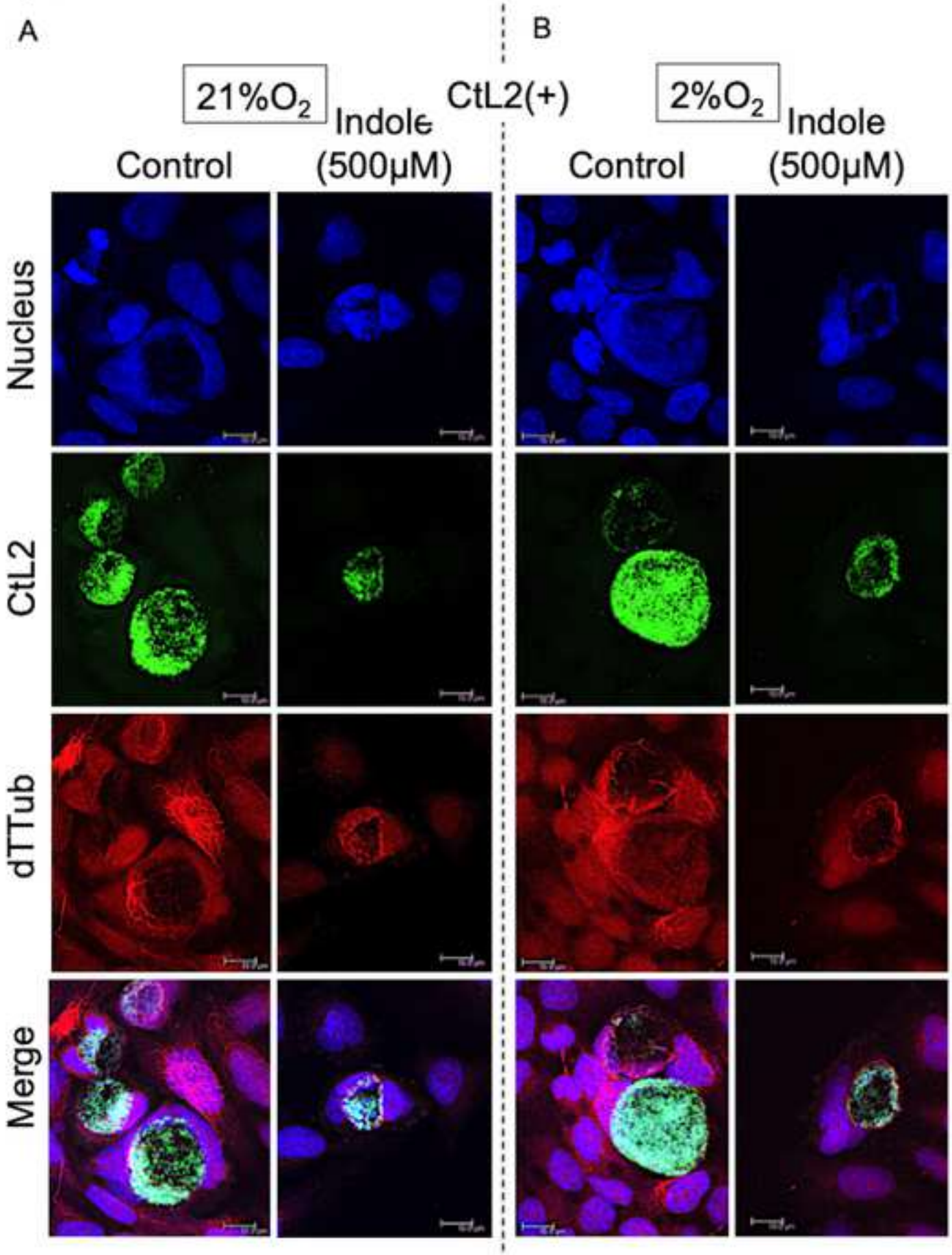

Figure6

Fig. 6

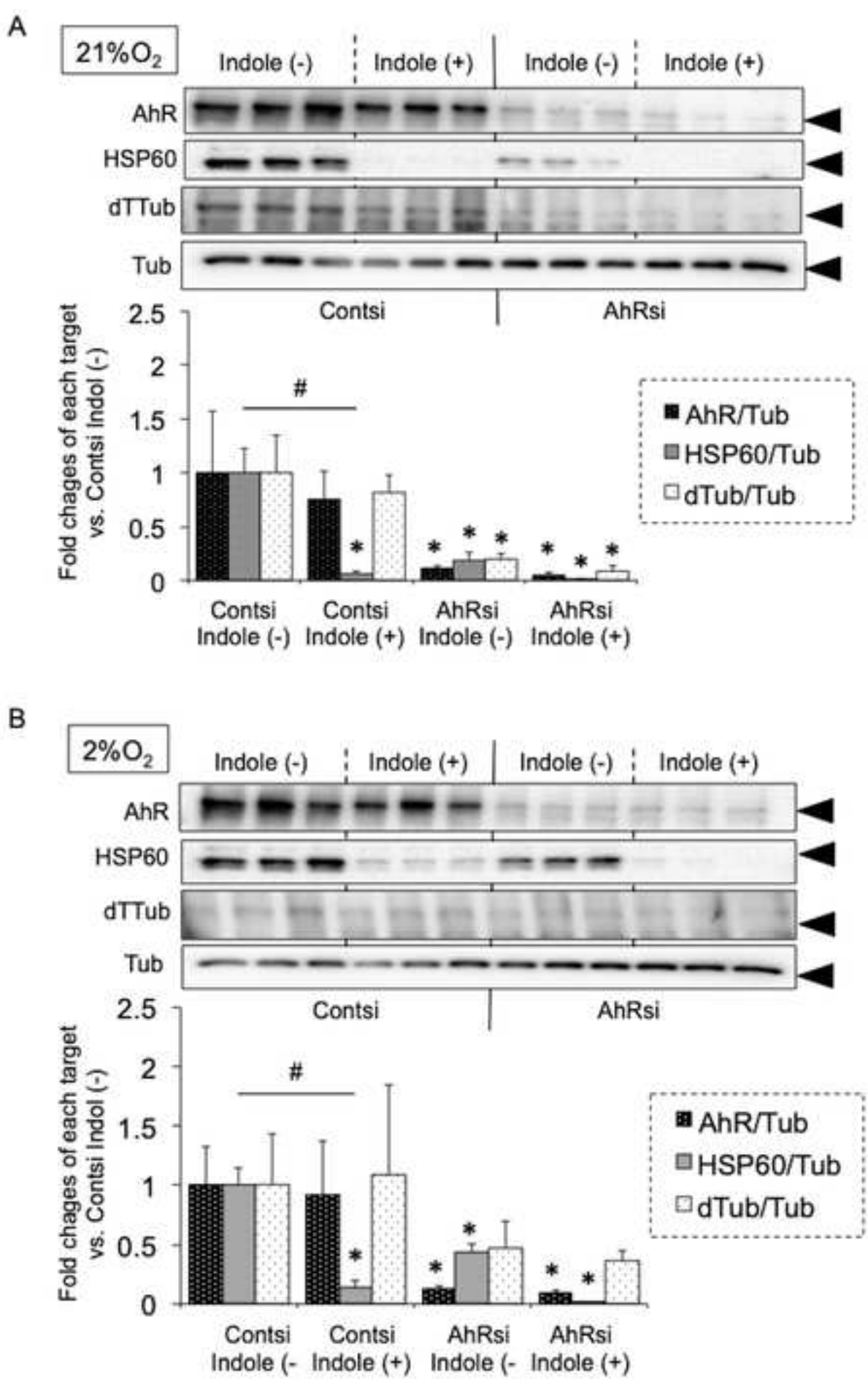

Figure7

Fig. 7